Bi-Level Scenario-Based Optimisation of Alternative Energy Systems for Inland Navigation

Richmond Anku, TU Delft, Delft/Netherlands, r.s.a.anku@tudelft.nl
Jeroen Pruyn, TU Delft, Delft/Netherlands, j.f.j.pruyn@tudelft.nl
Cornel Thill, TU Delft, Delft/Netherlands, c.h.thill@tudelft.nl

Abstract

This study investigates the implications of alternative energy adoption for inland vessels at both the system and operational levels. At the system level, hybrid powertrain sizing and energy demand estimation are based on confined-water hydrodynamics and expected operational profiles. At the operational level, scenarios of bunkering station distribution along discretised nodes of the Rotterdam - Antwerp corridor as a use case are analysed using a network-based approach coupled with mixed-integer linear programming (MILP). Results show that a vessel's operational profile and the spatial deployment of refuelling infrastructure strongly influence energy storage requirements. These insights provide a foundation for optimisation and trade-off analyses, supporting informed decision-making for the sustainable transition of inland navigation.

1. Background Literature

Vessel design for inland shipping is fundamentally a trade-off between operational range and cargo capacity, constrained by maximum dimensions. With conventional fossil-based propulsion systems, this trade-off is limited due to high energy density fuels such as diesel, which allow sufficient range without significantly reducing payload.

Existing research on alternative propulsion, power, and energy (PPE) systems for maritime and inland vessels has primarily focused on comparing technologies based on environmental impact, economic feasibility, and technological maturity. However, fewer studies address the optimisation and integration of onboard energy storage systems, which remain major challenges for inland shipping.

A key issue is the low volumetric and gravimetric energy density of alternative fuels such as hydrogen, ammonia, batteries, and methanol compared with diesel. These systems require significantly larger storage volume and additional weight to provide equivalent energy capacity. For gaseous fuels like hydrogen and ammonia, storage is further complicated by the need for cylindrical or spherical pressure vessels, which reduce space efficiency within conventional ship compartments.

Some studies have demonstrated the severity of these penalties. For example, *Taccani et al. (2020)* found that storing 140 kg of compressed hydrogen may require a storage system weighing approximately 1.8 tons. Similarly, hydrogen storage can lead to substantial deadweight losses, especially for pressurised systems, *Raucci and Calleya (2015), Zhaka and Samuelsson (2024)*. In retrofit applications, integrating non-rectangular storage tanks into existing ship layouts causes inefficient use of onboard space, while safety regulations impose strict compartmentalization requirements for batteries, methanol, and other fuels.

Other studies also concluded that volume constraints, weight penalties, and the resulting opportunity costs often influence technology selection more strongly than emissions performance itself, *Rivarolo et al. (2021)*. Payload loss directly reduces vessel revenue because cargo capacity is the primary economic function of cargo ships. Hydrogen-based solutions were found to cause particularly large revenue penalties due to reduced deadweight capacity, *Lagemann et al. (2022)*.

In modelling these impacts, *Hein et al. (2022)* proposed a probabilistic risk-averse method for energy storage sizing for a fully electric ship. With a Monte Carlo simulation, the authors generated varying operational profiles to account for uncertainties in voyage planning based on mission and payload constraints. *Li et al. (2023)* on another hand utilises an adaptive multi-objective approach for energy management and system sizing, aiming to achieve minimum investment cost and minimum battery degradation in a hybrid propulsion powertrain. Similarly, *Wang et al. (2025)* proposed a multi-objective optimisation method to balance ship endurance, cargo capacity utilisation, and emission reduction for bio-methanol hybridisation for container ships.

The existing optimisation studies have proposed approaches such as probabilistic sizing using Monte Carlo simulation, adaptive multi-objective optimisation for battery degradation and investment cost, and multi-stage optimisation frameworks integrating ship design and operational energy management. However, current approaches are largely developed for maritime shipping and do not adequately address the unique characteristics of inland waterway transport. In particular, they often neglect uncertainties associated with inland waterway conditions, variable power demand, operational profiles, and the limited availability and spatial distribution of bunkering infrastructure along inland corridors.

As a result, optimal energy system sizing and energy management are essential, especially for inland navigation where bunkering infrastructure may be sparse or unevenly distributed along the corridor. We therefore propose a bi-level scenario-based approach for sizing propulsion, power and energy systems for inland ships.

2. Methodology

The energy demand and required energy storage capacity of inland vessels vary significantly due to several interrelated factors. These include the vessel's hull form and hydrodynamic characteristics, which directly influence resistance and propulsion efficiency.

In addition, the availability and spatial distribution of bunkering or refueling infrastructure along the sailing corridor further affects onboard energy storage capacity requirement, since it constrains routing flexibility and dictates the minimum onboard energy required to ensure feasible operation between refueling points.

To estimate this and characterise the impacts of potential alternative fuels, we do so at both system and operational levels. At the system level, the energy demand and optimal hybrid powertrain sizing are estimated based on the hydrodynamics of the vessels, *Anku et al. (2025)* and component sizing methods, *Van Veldhuizen et al. (2025), Wang et al. (2021)*. And at the operational level, scenarios of bunkering availability and locations are explored to estimate the energy capacity requirements.

This methodology is based on the framework developed *Anku et al (2026)*.

2.1. System level energy converter sizing and optimisation

As described above, the shallow water hydrodynamic model is based on previous study detailed in *Anku et al. (2025)*.

$$R_T = R_T(V_{\text{stw}}, h_t, bf) \tag{1}$$

$$P_b = \frac{R_T \cdot V_{\text{stw}}}{\eta} \tag{2}$$

The objective of the system level optimisation is to minimise the total energy consumption of a hybrid propulsion configuration (internal combustion engine generator ICE-battery and fuel cell - battery). Objective:

$$\min \sum_{t \in T} \left(\frac{P_t^{\chi}}{\eta^{\chi}} - P_t^{\text{bat}} \right) \Delta t \tag{3}$$

$$P_t^{\chi} + \left| P_t^{\text{bat}} \right| = P_t^{\text{dem}} \tag{4}$$

$$P_t^{\chi} \leq S^{\chi}, \quad \forall t \in T \tag{5}$$
$$0.2 \cdot C^{bat} \leq SoC_t \leq 0.8 \cdot C^{\mathrm{bat}}, \quad \forall t \in T \tag{6}$$

$$SoC_t = \begin{cases} SoC_0 - \eta_{bat} P^{bat}{}_t \, \Delta t, \ t = 1 \\ SoC_{t-1} - \eta_{bat} \, P^{bat}{}_t \, \Delta t, \ t > 1 \end{cases} \tag{7}$$

Decision variables:

P_t^{χ} instantenous power of energy converter (kW), $\chi \in$ {ice,fc},
P_t^{bat} instantenous battery power (kW),
SoC_t instantenous state of charge of battery (kWh),
S^{χ} rated capacity of energy converter (kW),
C^{bat} rated capacity of battery (kWh).

2.2. Operational scenario of bunkering infrastructure distribution

The objective of the operation level submodel is to minimise the energy capacity and the total sum of refuelling cost

Objective:

$$\min \quad E + \sum_{i \in N} \overline{c_i} \cdot w_i \tag{8}$$

Constraints:

Energy flow balance $i \in N \setminus \{s, t\}$

$$\sum_{j:(j,i) \in A} x_{ji} = \sum_{j:(i,j) \in A} x_{ij} = 1 \tag{9}$$

To enforce a sequential order of vessel visiting node along the corridor and eliminating subtours, we adopted the Miller-Tucker-Zemlin (MTZ) formulation, *Campos et al. (2025), Lyu et al. (2024),* which eliminates This constraint is modelled as:

$$u_j \geq u_i + 1 - |N|(1 - x_{ij}) \tag{10}$$

Subtour bounds

$$1 \leq u_i \leq |N| - 1 \tag{11}$$

Energy level bounds and refuelling limits at bunkering nodes

$$\delta E \leq y_i \leq E \tag{12}$$
$$w_i \leq E - y_i \tag{13}$$

To ensure the conservation of energy levels across arcs in the vessel's route, accounting for energy consumption and refueling, while accommodating the binary arc selection variable x_{ij}, the energy balance ($(i, j) \in A$) is given by:

$$y_j \leq y_i + w_i - e_{ij} + M(1 - x_{ij}) \tag{14}$$
$$y_j \geq y_i + w_i - e_{ij} - M(1 - x_{ij}) \tag{15}$$

M is a constant used to relax the constraints for arcs not selected in the route, ensuring the feasibility of the MILP formulation. And the minimum energy level at the destination:

$$y_t \geq \delta E$$

Decision Variables:

$E \geq 0$ Energy capacity (kWh),
$x_{ij} \in \{0,1\}$binary indicator of leg usage,
$y_i \geq 0$ energy level (kWh) at node $i \in N$,
$w_i \geq 0$ energy refilled (kWh) at node $i \in C$
$e_{ij} \geq 0$ energy consumption (kWh) on (i,j)
$\bar{c}_i \geq 0$ unit refuelling cost (€/kWh) at node
$\delta \in (0,1)$ minimum energy reserve
$u_i \geq 0$subtour elimination variable for $i \in N\backslash\{s\}$

3. Results and Discussion

This methodology was applied to a Class VI (M8) inland vessel operating on the Rotterdam–Antwerp corridor. The choice of case study is supported by inland shipping traffic data from Rijkswaterstaat, which shows that the Rotterdam–Antwerp route represent the most frequently sailed corridor in the dataset as shown in Fig.1.

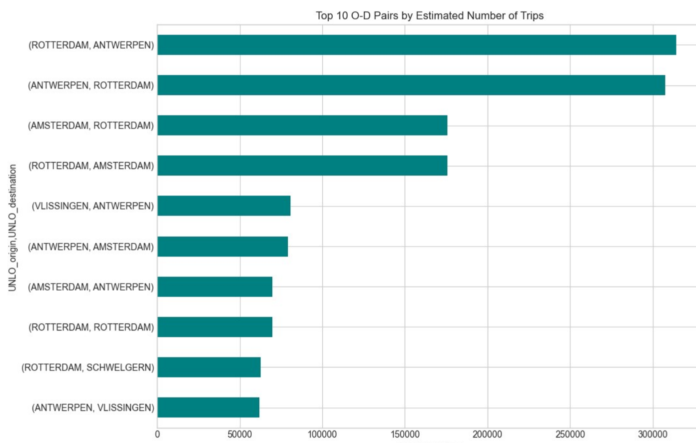

Fig.1: Top 10 inland waterway origin–destination (O-D) pairs ranked by estimated frequency of trips

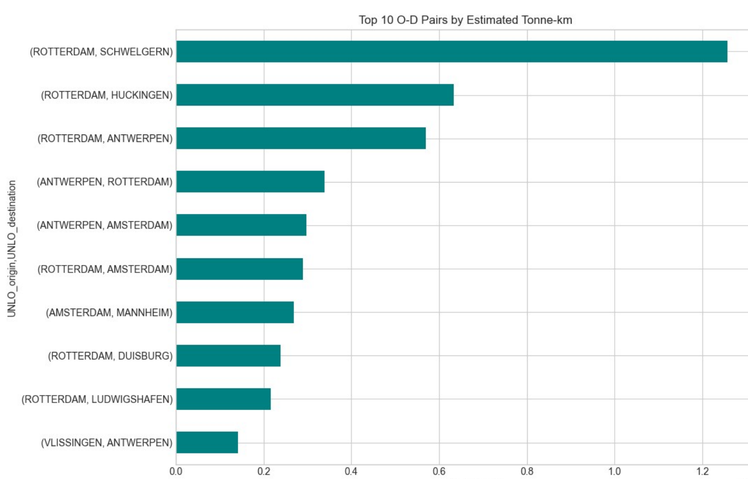

Fig.2: Top 10 inland waterway origin–destination (O-D) pairs ranked by estimated t-km transported

In terms of voyage frequency, this corridor accounts for ~42% of total recorded trips, indicating its strong operational dominance in inland navigation. Although when evaluating transport work in terms of tonne-kilometres, highest freight flows are directed from Rotterdam towards the Duisburg area including Schwelgern, Huckingen, and Duisburg, along the Rhine corridor. This segment accounts for ~48% of total transport work, Fig.2. This difference is primarily driven by longer sailing distances and the use of larger vessel classes operating on the Rhine route.

A closer look of the vessel class distribution, as shown in Fig.3, indicates a clear difference in fleet composition between the two corridors. On the Rotterdam–Antwerp corridor, the dominant vessel class is M8, corresponding to Class Va vessels, reflecting the high-frequency operation of medium-sized inland ships on this route. In contrast, the Rotterdam–Duisburg (Schwelgern) corridor is primarily served by M9 vessels, corresponding to Class VI large Rhine vessels.

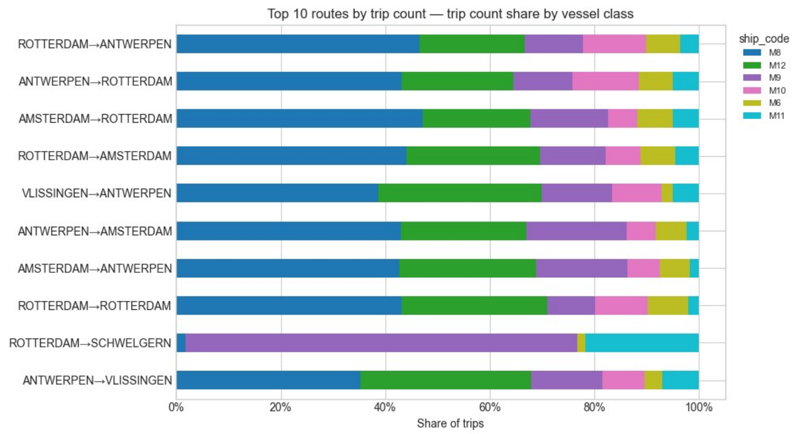

Fig.3: Share of inland vessel classes per shipping route

3.1. Power Profile and Energy Consumption

Now from the considered corridor for this work (Rotterdam – Antwerp), we discretise the voyage into nodes, made up of terminals, ports and locks. The segments between nodes are characterised by the waterway properties, which influence the power demand, particularly the confinement effects of the waterway (depth and width). The discrete nodes are Rotterdam (port) → Moerdijk (terminal) → Volkeraksluizen (lock) → Bergen op Zoom (terminal) → Kreekraksluizen (lock) → Antwerp (port).

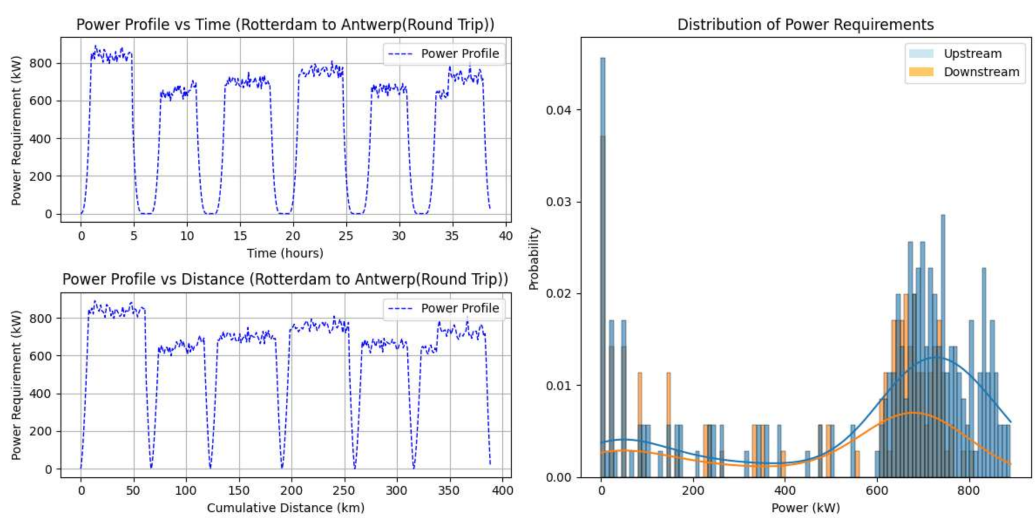

Fig.4: Power Profile (Return Voyage Rotterdam - Antwerp)

The propulsion power demand for a round trip between Rotterdam and Antwerp, together with the vessel's speed relative to water and ground, is shown in Figs.4 and 5. The results indicate that hydrodynamic current effects are relatively limited on this corridor compared to the Rhine. Most importantly sections of this corridor are canalized due to the presence of locks, therefore the most predominant effects would be tidal effects particularly on the Nieuwe Maas within Rotterdam area open to the sea and Scheldt river within Antwerp area also open to the sea. Notably, the presence of two locks on this corridor necessitates about 45 minutes of waiting time where propulsion power demand of necessity would be zero, as can be seen in the power profile, this waiting is time at Volkeraksluizen and Kreekraksluizen are accounted for in this model.

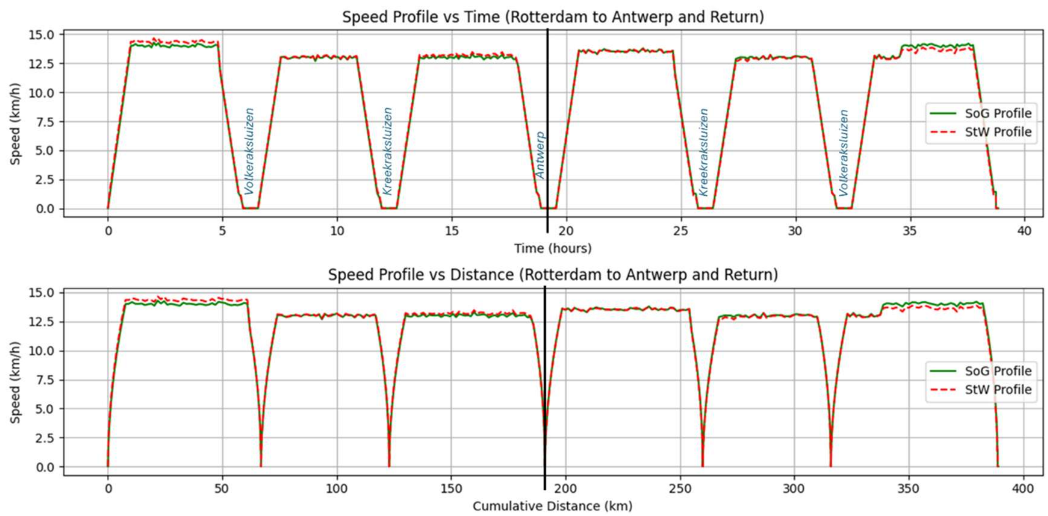

Fig.5: Ship speed profile (Return Voyage Rotterdam - Antwerp)

The energy consumption between nodes of the vessel in the outbound voyage is marginally more than the return voyage, Fig.6, as expected, due to tidal effects on the waterway although not significant as highlighted earlier. Also, the loading condition of the vessel plays an important role here, accounting for full full-loaded condition outbound and the partly loaded condition on the return.

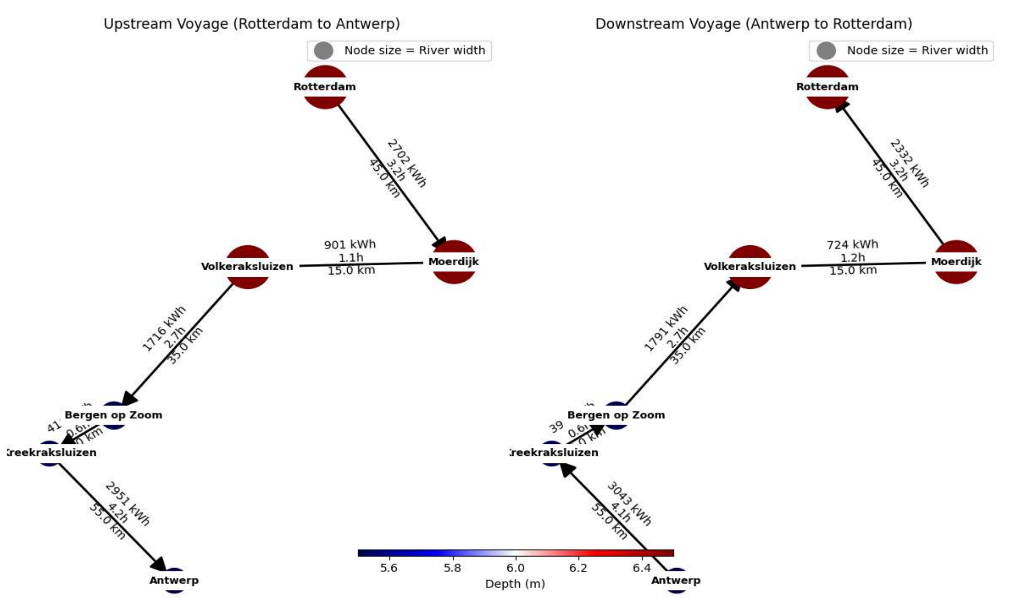

Fig.6: Energy Consumption on discrete nodes (Return Voyage Rotterdam - Antwerp)

3.2. System Level Sizing Optimisation (ICE-battery and Fuel Cell-battery configuration)

Applying the proposed power management methodology to both the ICE–battery and FC–battery powertrain configurations, the resulting propulsion power balances and instantaneous operating efficiencies over the voyage are presented in Figs.7 and 8. The FC–battery configuration, Fig.7, produced a smooth fuel cell power output that tracked the demand profile gradually, with the battery absorbing residual fluctuations through deep but cyclically balanced charge–discharge. FC efficiency varied across the voyage in line with load, ranging from approximately 0.52 to 0.65.

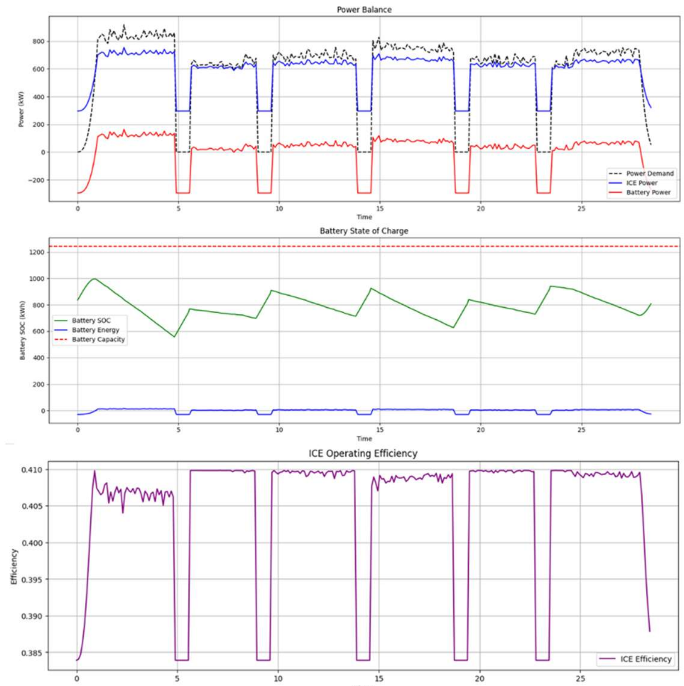

Fig.7: Optimised operation strategy for ICE-Battery configuration

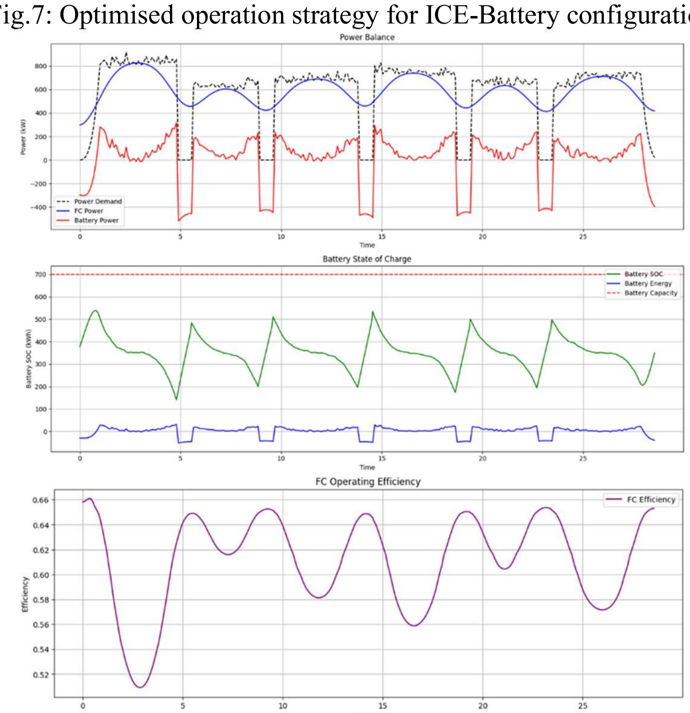

Fig.8: Optimised operation strategy for Fuel cell - Battery configuration

Table I: Sized Energy converters and battery

	ICE-Battery	FC-Battery
Energy converter size (kW)	750	820
Battery capacity (kWh)	1240	700
Operating efficiency	0.38 – 0.41	0.52 – 0.65
Maximum battery charge (kW)	164	318
Maximum battery discharge (kW)	295	520

In contrast, the ICE–battery configuration, Fig.8, operated the engine in discrete high-efficiency load blocks, with the battery providing relatively stable buffering throughout. This strategy required a significantly larger battery capacity of approximately 1200 kWh against 700 kWh for the fuel cell (FC) system to support the internal combustion engine (ICE) generator operating strategy, although with converter capacity of about 750 kW against 820 kW of fuel cell. Overall, the FC–battery configuration achieved smoother operation and deeper battery utilisation, while the ICE–battery system relied on a larger battery buffer operating at shallower cycles.

3.3. Operational level Refuelling Scenarios

The operational level examines how different spatial arrangements of bunkering infrastructure along the Rotterdam → Antwerp corridor affect onboard energy storage requirements and operational costs. Three scenarios with three bunkering stations are considered: Rotterdam–Bergen op zoom–Antwerp, Rotterdam–Moerdijk–Bergen op zoom, and Rotterdam–Volkersluizen–Antwerp, Fig.9.

The vessel is modelled using a forward-looking decision rule in which it estimates the energy required to reach the next node and determines whether that node is a bunkering station. Based on this assessment and its current energy state, it adjusts its initial storage level to ensure that the selected bunkering configuration remains feasible. Upon arrival at a bunkering node, the vessel replenishes only the energy required to guarantee reachability of the next available refueling station. As a result, the bunkered quantity is not fixed but depends on expected energy consumption, spacing between bunkering nodes, and spatial variation in fuel prices.

The comparison of the three scenarios shows that the spatial distribution of bunkering points directly influences required onboard energy storage capacity. In the scenario with wider spacing between stations (Rotterdam–Moerdijk–Bergen op zoom), the vessel must maintain a higher minimum energy reserve to ensure it can reach the next refueling opportunity. In contrast, the Rotterdam–Volkersluizen–Antwerp configuration reduces spacing between key nodes, leading to lower required onboard storage capacity, Fig.9. Overall, the results demonstrate that bunkering infrastructure layout is a key determinant of both energy system sizing and operational feasibility in inland waterway transport.

3.4. Energy Storage Capacity Sizing

The analysis compares onboard storage requirements for methanol, hydrogen, LNG, and HVO by first considering only their basic energy densities and then extending the evaluation to include a packaging factor that accounts for storage geometry and safety systems.

Results show that when only volumetric and gravimetric energy densities are considered, the fuels differ mainly in intrinsic energy content. However, once storage constraints are included, the effective space and weight requirements increase significantly.

Gaseous and cryogenic fuels such as hydrogen and LNG are most affected because they require cylindrical, spherical pressure or cryogenic tanks, which introduce additional unused space when installed in conventional ship hull geometry. These systems also require extensive safety equipment (insulation, venting, pressure relief, leak detection), further increasing both weight and volume demand.

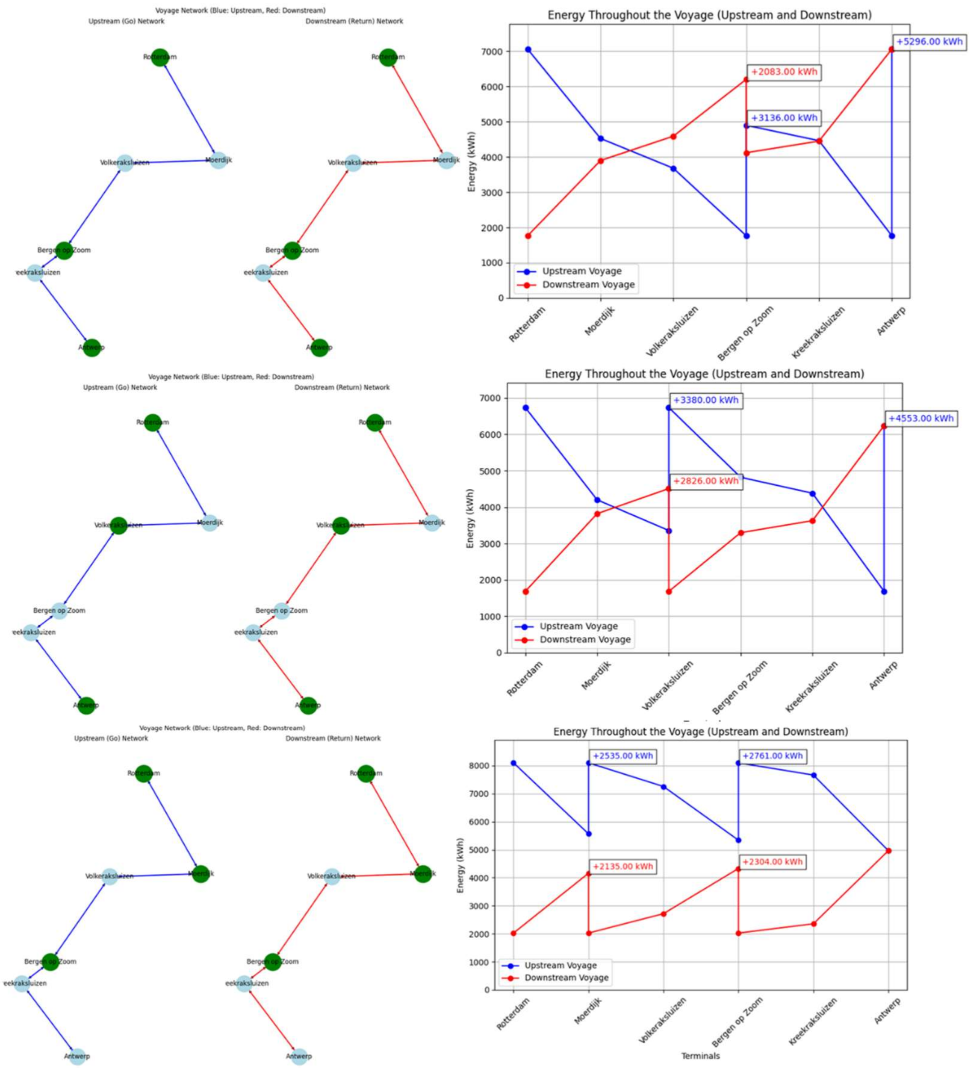

Fig.9: Scenarios of distribution of bunkering infrastructure along the Rotterdam - Antwerp corridor

Methanol, while easier to store as a liquid in conventional tanks, still requires notable space penalties due to safety requirements such as cofferdams and dedicated ventilation systems separating it from other compartments.

4. Conclusions and Recommendations

This paper presents a methodology for estimating alternative energy storage requirements for inland vessels by integrating hydrodynamics, operational constraints, hybrid powertrain sizing, and bunkering infrastructure into a unified framework. The results demonstrate that vessel performance, and energy consumption strongly influenced not only by the propulsion technology itself, but also by river conditions and the availability of bunkering infrastructure along the sailing corridor.

The comparison of hybrid powertrains revealed that the ICE–battery configuration operated the engine in discrete load blocks, requiring larger battery buffer (1200 kWh) to manage transients and peak loads, while maintaining a stable efficiency band throughout. The FC–battery configuration operated at higher efficiency at cruise but showed greater efficiency variation with load particularly during lock transits and required a significantly smaller battery capacity (700 kWh) with deeper charge–discharge cycling.

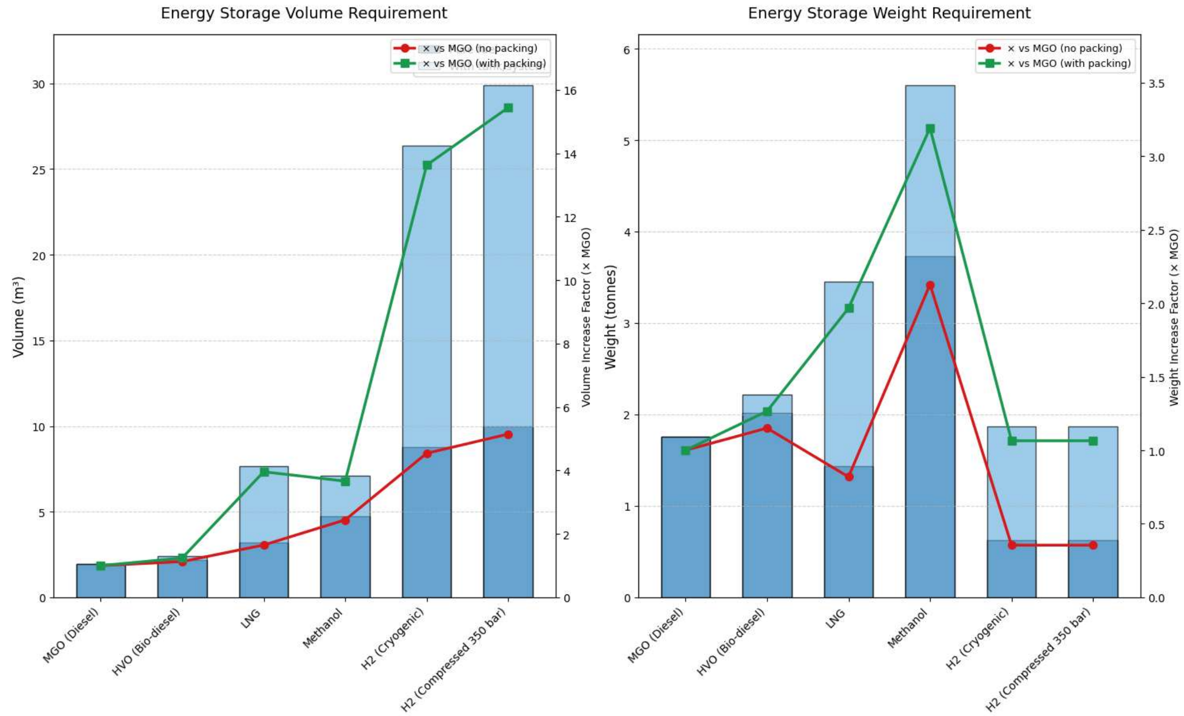

Fig.10: Volume and Mass requirements for Alternative Fuels

The analysis also revealed that bunkering infrastructure plays a critical role in determining onboard storage requirements and operational feasibility. Larger distances between bunkering stations increase the required onboard energy capacity, while regional fuel price differences introduce non-linear cost impacts. Multi-scenario analysis identified bunkering availability as one of the most influential factors affecting system feasibility.

Furthermore, the comparison of alternative fuels highlighted that onboard storage volume and weight are major design constraints, particularly for hydrogen due to its low energy density and large storage requirements. Other fuels such as LNG, methanol, and HVO present different trade-offs between storage, cost, and operational performance.

To conclude, this methodology provides a scenario-based framework for sizing alternative energy systems under operational constraints and uncertainty, supporting the design of sustainable inland waterway vessels.

Acknowledgements

This research is conducted within the PATH2ZERO project, co-funded by NWA L2-Thema 2020 Zero emission shipping (ZES) program by Netherlands Organization for Scientific Research (NWO) with Grant NWA.1439.20.001, and by the Temporary research subsidy scheme Top Sector Logistics 2022-2026 of the Ministry of Infrastructure and Water Management.

References

ANKU, R.; PRUYN, J.; THILL, C. (2024), *A Review of the State-of-the-Art Sustainable and Climate-Resilient Inland Waterway Vessels*, Int. Marine Design Conf., https://doi.org/10.59490/imdc.2024.826

ANKU, R.; PRUYN, J.; THILL, C. (2025), *Towards Climate Resilient Inland Waterway Vessel Design: Concept of Distributed Thrust for Shallow Water Conditions*

CAMPOS, R.; COELHO, L.C.; MUNARI, P. (2025), *New Formulations for the Robust Vehicle Routing Problem with Time Windows Under Demand and Travel Time Uncertainty*, OR Spectrum 47/2, pp.411–453, https://doi.org/10.1007/s00291-024-00781-z

CORADDU, A.; GIL, A.; AKHMETOV, B.; et al. (2022), *Energy Storage on Ships*, Sustainable Energy Systems on Ships, Elsevier

HEIN, K.; XU, Y.; ADITYA, V.; GUPTA, A.K. (2022), *A Probabilistic Risk-Averse Approach for Energy Storage Sizing in All-Electric Ship*, J. Energy Storage 55, https://doi.org/10.1016/-j.est.2022.105392

LAGEMANN, B.; LINDSTAD, E.; FAGERHOLT, K.; RIALLAND, A.; ERIKSTAD, S.O. (2022), *Optimal Ship Lifetime Fuel and Power System Selection*, Transport and Environment 102, https://doi.org/10.1016/j.trd.2021.103145

LI, X.; HUANG, J.; ZHANG, J.; et al. (2023), *An Adaptive Multi-Objective Joint Optimization Framework for Marine Hybrid Energy Storage System Design Considering Energy Management Strategy*, J. Energy Storage 68, https://doi.org/10.1016/j.est.2023.107689

LYU, Z.; ISLAM, M.Z.; YU, A.J. (2024), *A Scalable and Adaptable Supervised Learning Approach for Solving the Traveling Salesman Problems*, IEEE Transactions on Intelligent Transportation Systems 25/11, pp.17092–17104, https://doi.org/10.1109/TITS.2024.3410691

RAUCCI, C.; CALLEYA, J. (2015), *Hydrogen on Board Ship: A First Analysis of Key Parameters and Implications*

RIVAROLO, M.; RATTAZZI, D.; MAGISTRI, L.; MASSARDO, A.F. (2021), *Multi-Criteria Comparison of Power Generation and Fuel Storage Solutions for Maritime Application*, Energy Conversion and Management 244, https://doi.org/10.1016/j.enconman.2021.114506

TACCANI, R.; MALABOTTI, S.; DALL'ARMI, C.; MICHELI, D. (2020), *High Energy Density Storage of Gaseous Marine Fuels: An Innovative Concept and Its Application to a Hydrogen Powered Ferry*, Int. Shipbuilding Progress 67/1, pp.33–56, https://doi.org/10.3233/ISP-190274

VAN VELDHUIZEN, B.N.; VAN BIERT, L.; ÜNLÜBAYIR, C.; VISSER, K.; HOPMAN, J.J.; ARAVIND, P.V. (2025), *Component Sizing and Dynamic Simulation of a Low-Emission Power Plant for Cruise Ships with Solid Oxide Fuel Cells*, Energy Conversion and Management 326, https://doi.org/10.1016/j.enconman.2024.119477

WANG, X.; SHIPURKAR, U.; HASELTALAB, A.; POLINDER, H.; CLAEYS, F.; NEGENBORN, R.R. (2021), *Sizing and Control of a Hybrid Ship Propulsion System Using Multi-Objective Double-Layer Optimization*, IEEE Access 9, pp.72587–72601, https://doi.org/10.1109/ACCESS.2021.-3080195

WANG, Y.; ZHANG, C.; SHI, Y. et al. (2025), *A Synergistic Multi-Energy System for Carbon-Neutral Container Ships via Green Methanol-Biomass Hybridization (GMB-CCHP)*, Energy 329, https://doi.org/10.1016/j.energy.2025.136767

WANG, Y.; WRIGHT, L.A. (2021), *A Comparative Review of Alternative Fuels for the Maritime Sector: Economic, Technology, and Policy Challenges for Clean Energy Implementation*, World 2/4, pp.456–481, https://doi.org/10.3390/world2040029

ZHAKA, V.; SAMUELSSON, B. (2024), *Hydrogen as Fuel in the Maritime Sector: From Production to Propulsion*, Energy Reports 12, pp.5249–5267, https://doi.org/10.1016/j.egyr.-2024.11.005

ZHANG, W.; HE, Y.; WU, N. et al. (2023), *Assessment of Cruise Ship Decarbonization Potential with Alternative Fuels Based on MILP Model and Cabin Space Limitation*, J. Cleaner Production 425, https://doi.org/10.1016/j.jclepro.2023.138667